Photodetachment of Deprotonated Aromatic Amino Acids: Stability of the dehydrogenated radical depends on deprotonation site

Jennifer Anna Noble, Juan Aranguren-Abate, Claude Dedonder, Christophe Jouvet, Gustavo Pino

Photodetachment of Deprotonated Aromatic Amino Acids: Stability of the dehydrogenated radical depends on deprotonation site

Jennifer Anna Noble*, Juan P. Aranguren-Abate, Claude Dedonder, Christophe Jouvet, Gustavo A. Pino

a- PIIM: UMR-CNRS 7345, Aix-Marseille Univ. Avenue Escadrille Normandie-Niémen 13397 Marseille cedex 20, France. jennifer.noble@univ-amu.fr

b- INFIQC: Instituto de Investigaciones en Fisicoquímica de Córdoba (CONICET – UNC) - Haya de la Torre y Medina Allende, Ciudad Universitaria, X5000HUA Córdoba, Argentina.

c- Departamento de Fisicoquímica, Facultad de CienciasQuímicas– Universidad Nacional de Córdoba – Haya de la Torre y Medina Allende, Ciudad Universitaria, X5000HUA Córdoba, Argentina.

d- Centro Láser de Ciencias Moleculares - Universidad Nacional de Córdoba - Haya de la Torre s/n, Pabellón Argentina,Ciudad Universitaria, X5000HUA Córdoba, Argentina.

Abstract

While aromatic amino acids in their deprotonated form have been well characterized by IR and photoelectron spectroscopies, no information is available on the neutral dehydrogenated protonated radicals and, in particular, on their stability when the deprotonation site is changed. This is investigated by observing the neutral fragment issued from either simple photodetachment or dissociative photodetachment of the deprotonated aromatic amino acids phenylalanine, tyrosine, and tryptophan. We show that the dehydrogenated radicals of aromatic amino acids produced upon photodetachment of molecules deprotonated on the carbonyl group dissociate without barrier, leading to the formation of CO_2 and a radical amine. However, when the system is deprotonated on functional groups located on the chromophore, the radicals produced by photodetachment are stable, indicating the important photostabilizing role played by functional groups.

Introduction

There are three aromatic amino acids: phenylalanine (Phe), tyrosine (Tyr), and tryptophan (Trp).

Though seemingly simple species, fundamental questions regarding the gas-phase structure of deprotonated amino acids and, in particular, the neutral radicals issued from their electron detachment remain unanswered to date. The stability of small dehydrogenated acid radicals has been studied through coincidence techniques[1]. In particular, it has been shown that the simplest, acetyloxyl, loses CO_2 upon photodetachment, with a small barrier (0.1eV)calculated for CO_2 loss[2].

The most favorable protonation or deprotonation site in aminoacids is a recurring question in experiments involving electrospray ionization (ESI), addressed by means of IRMPD spectroscopy [34] or photoelectron spectroscopy[5]. The photodetachment spectrum of deprotonated tryptophan$[Trp\text{-}H]^-$ has been studied at room temperature by Compagnon et al.[6]. A threshold at 315nm (3.94eV, 31750cm^{-1}) was observed and assigned to the carboxylate anion.The photoelectron spectrum obtained by Tian etal.[5]demonstrated the competition between two deprotonation sites in tyrosine, leading to either the carboxylate or phenoxide anions. More recently, it has been shown that the preferred protonation or deprotonation site is totally dependent on the (uncontrollable) ESI conditions[7]. More dramatically, it has been shown, in the case of p-hydroxybenzoic acid produced by ESI, that populations of the thermodynamically less favored gaseous carboxylate anionor the thermodynamically more favored gaseous phenoxide anion can be varied back and forth by changing the probe position, capillary voltage, desolvation-gas temperature, sample infusion flow rate, and cone voltage[8]. From these works it can be concluded that there is no clear relationship between the observation of a given isomer and its relative stability; thus this topic will not be discussed in this paper.

The collision induced dissociation (CID)of $[Trp\text{-}H]^-$has been studied[910] and the observed fragments derive mainly from the fragmentation of the peptide side chain.

In a recent paper[11] we have shown that in deprotonated naphthoate anions there is a competition between ionic fragmentation in the electronically excited anion and electron detachment. This is not observed in benzoate since the excited states of the deprotonatedbenzoate anion are higher than those of naphthoate and lie above the adiabatic detachment energy (ADE).Once above the photodetachment energy, one can observe the simple photodetachment of the anion leaving the stable radical, but at higher energies the radical loses CO_2 through an exit barrier along the C-CO_2 bond which has been measured at 0.5eV[11].

Recently, the indolide anion has been characterized and its adiabatic detachment energy (ADE) = 2.43 eV was measured through photoelectron spectroscopy[12]. Since the excited states of indole are also low in energy compared to those in phenol or benzene, one might expect to see competition between ionic fragmentation and photodetachment, as for naphthoate.

The questions we will answer in this paper are:

. How does the stability of the dehydrogenated (deprotonated, then electron detached) radical change with the deprotonated site?

. Is there a competition between photofragmentation of the anion and its photodetachment?

. Is there a fragmentation in the radical after photodetachment and, if so, is there a barrier to the fragmentation?

. What is the Influence of the amino acid side chain on the electron binding energy of the deprotonated chromophore?

Experimental

The experimental setup used for cold ion photofragmentation spectroscopy has been described in previous publications131415and has recently been modified to detect negative ions and neutral particles11.Deprotonated phenylalanine, tyrosine, and tryptophan were produced in the electrospray ionization (ESI) source by injecting a solution of amino acid at 10-4 M in 5:1 mixture of methanol:water.

The ions produced in the ESI are injected into the cryogenic ion trap just after a helium pulse has been introduced. The ions are stored in the cold trap for a few tens of ms, the time necessary for cooling to c.a. 30 K and subsequent reduction of the pressure in the trap. The ions are then extracted and accelerated at 3.0 kV. The voltage of the extracting electrode of the trap and the accelerating grid are adjusted to fulfill the Wiley McLaren focusing conditions[16]. After the accelerating grid, the ions enter the Gauss tube set at the accelerating grid potential and, once they are inside, the tube is switched to ground. The ions then travel in the field free region of the time of flight (TOF) mass spectrometer with a kinetic energy due to the accelerating voltage and they are referenced to the ground potential. After 1m of flight, they enter the post accelerating/decelerating "box". The ions (or neutrals) are detected after the "box" with a MCP detector[17].

The laser used for photodissociation or photodetachment of the ions is a tunable OPO laser (EKSPLA) (10 Hz repetition rate, 10 ns pulse width, and a spectral resolution of ~ 10 cm^{-1}). The laser can interact with the ions in two different parts of the setup (see supplementary information): either in the ion trap, which allows monitoring of the photodissociation process leading to a daughter ion and a neutral fragment by extracting the ions after the laser shot, or in the Gauss tube. In the latter case, since the parent ions have been accelerated, the neutral parent radicals produced after photodetachment and/or the neutral daughter fragments can be detected by the MCP. The intact parent radical will arrive at the same time as the anion precursor and the signal will be as narrow as the anion signal. In contrast, the neutral fragments will travel with the kinetic energy of the parent ion plus the kinetic energy (positive or negative) released in the dissociative process, so that they will

be observed at the same time-of-flight as the parent but exhibiting peak broadening due to the kinetic energy release.

To discriminate between the parent anion and the parent neutral photodetached radical, two methods can be used:

a) Decelerating the anions by applying high voltages (1.2 kV) in the accelerating/decelerating "box" (when a negative voltage is applied, the ions are decelerated in the box and will travel slower than the neutrals, thus arriving at the detector after the neutrals).

b) Leaving the voltage on the Gauss tube in order to decelerate the anions at the output of the tube and prevent them reaching the detector, while the neutrals are not perturbed. This method minimizes the time and the distance travelled by the parent ions and thus minimizes the background signal from neutral fragments produced by collisions of the parent ions with the residual gas.

Calculations

Simple calculations using the density functional theory (DFT) with the B3LYP functional as implemented in the Turbomole software[18] with the aug-cc-pVTZbasis set[19] were performed to determine the ADE and vertical detachment energy (VDE)as well as the dissociation energy of the photodetached radical.

The ground states of the neutral and the deprotonated and protonated ions[20] have previously been calculated in the case of Trp. For the deprotonated anion $[Trp-H]^-$, similar calculations have been performed by Compagnon et al.[6] and the most stable structure has been determined to be the one in which the carboxylate lies above the indole plane. Similar starting geometries have been used in the case of $[Phe-H]^-$ and $[TyrH]^-$ as the starting point of our calculations (see S.I. for the xyz coordinate of optimized structure).

Results

a) Photodissociation in the ion trap

None of the deprotonated aromatic amino acids led to the production of any ionic fragment when the interaction with the laser took place in the ion trap, indicating that there are no optically accessible excited states below the photodetachment threshold, in contrast with the case of naphthoate (Pino et al. 2019).

b) Photodetachment in the Gauss tube

$[Phe-H]^-$ anion

As presented in the experimental section, intact radicals appear as narrow peaks while fragments appear as broadened peaks. For deprotonated phenylalanine $[Phe\text{-}H]^-$, only two broad peaks are observed in the TOF mass spectra of neutrals, without any signature of a narrow component, indicating that the phenylalanyl radical is unstable above the photodetachment threshold (Figure1).

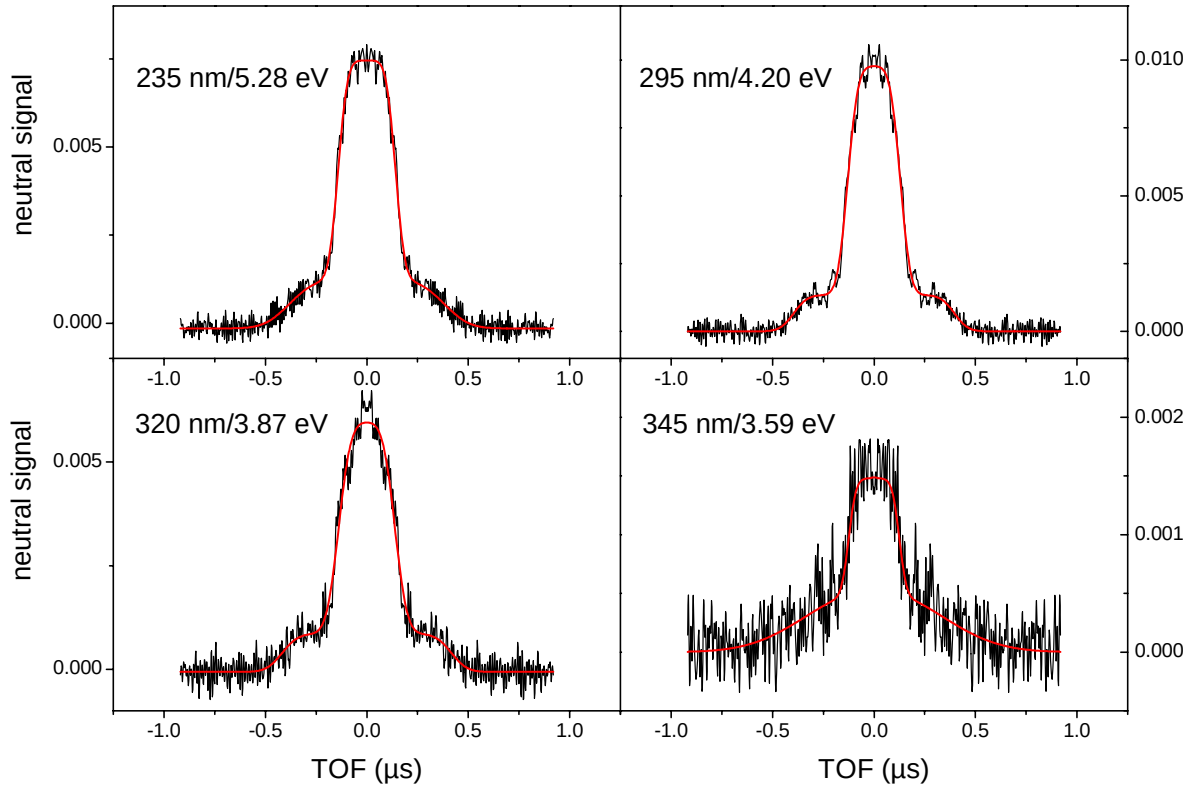

Figure 1. Time of Flight peak profiles obtained at different excitation energies. The profiles have been symmetrized (see supplementary information) and are fitted with two combinations of erf functions with different widths for the fragments.

The peak profiles were symmetrized and fitted assuming two combinations of erf functions for two fragments (see supplementary information for the fitting procedure).The mean widths of the two broad peaks (140 ± 10 ns and 405 ± 35 ns) remain unchanged as a function of the excitation energy(Figure 1 and supplementary information). The ratio of the widths of the two broad peaks should reflect the mass ratio of the two neutral fragments. If we assume that the dissociation channel corresponds to CO_2 loss, as in aryl acids[11], the ratio of the fragments masses is 0.37. The ratio of the experimental widths is 0.35 ± 0.05, in agreement with the mass ratio for the CO_2 loss channel.

Considering the widths of the peaks and the geometry of the TOF mass spectrometer, we can extract the kinetic energy released in the dissociation process, which is 0.21 ± 0.02 eV.(See S.I.)

Since the phenylalanyl radical fragments upon photodetachment, the photodetachment and photofragmentation thresholds are the same. The thresholds were determined to be 3.54 ± 0.02 eV (350±2 nm)by scanning the laser while monitoring the intensity of the neutral fragment peak at mass 120 (Figure 2).

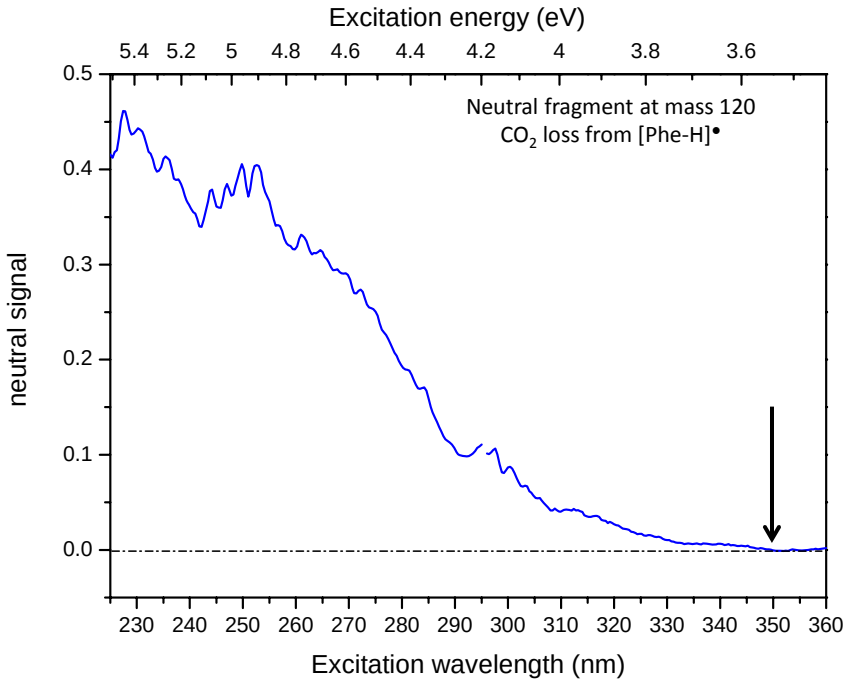

Figure 2.Excitation spectrum recorded while detecting the neutral fragment at mass 120 [Phe-H-CO_2]•.

[Tyr-H]⁻ anion

The TOF mass spectra corresponding to neutrals produced after photodetachment of the anion, either intact tyrosyl radicals appearing as a narrow peak or its fragments (broadened peaks), were recorded at different excitation energies (Figure 3).

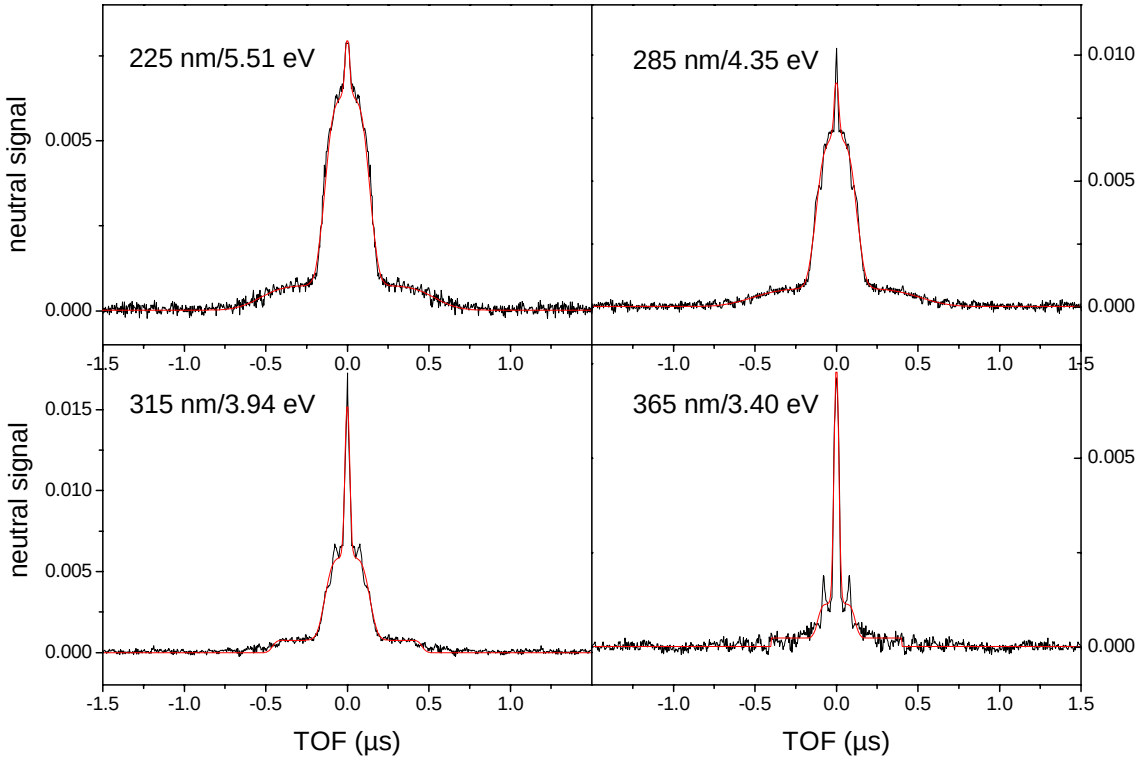

Figure 3. Time of Flight peak profiles obtained at different excitation energies for [Tyr-H]$^-$. The profiles have been symmetrized and are fitted with a sum of a Gaussian function for the narrow peak (tyrosil radical) and a combination of two erf functions of different widths for the fragment peaks (see supplementary information for the symmetrization and fitting procedure).

The intensity of the narrow peak decreases relative to that of the broad peaks as the energy increases, indicating that the fragmentation channel yield increases. The peak profiles were symmetrized and fitted assuming two combinations of erf functions for the two fragments and a Gaussian function for the tyrosyl narrow peak (*see supplementary information for the fitting procedure)*. The width of the narrow peak is the same as the width of the parent anion peak, i.e. 20 ns. As for phenylalanyl, the widths of the broad peaks remain unchanged as a function of the excitation energy. In this case, the mean widths of the broad peaks are (135 ± 15) ns and (480 ± 30) ns, the ratio being (0.28 ± 0.05), in agreement with the mass ratio of 0.32 obtained if we assume that the dissociation channel corresponds to CO_2 loss, as for [Phe-H]$^-$.From the widths of the fragment peaks, we can then extract the kinetic energy released in the dissociation process, which is 0.21 ± 0.04 eV.

The photodetachment and fragmentation thresholds were determined by scanning the laser while monitoring the intensity of the narrow and the broad part of the peak profile, respectively. The photodetachment threshold for $[Tyr\text{-}H]^-$(Figure 4) is observed at 2.58 ± 0.03 eV (480 ± 5 nm) and corresponds to the ADE observed by Tian et al. for the $TyrO^-$ anion. The fragmentation signal rapidly increases above 3.54 ± 0.05 eV, which corresponds to the experimental ADE for the $TyrCO_2^-$ anion observed by Tian et al., and there is also a weak fragmentation signal increasing slowly from 3.10 ± 0.05 eV to 3.54 eV.

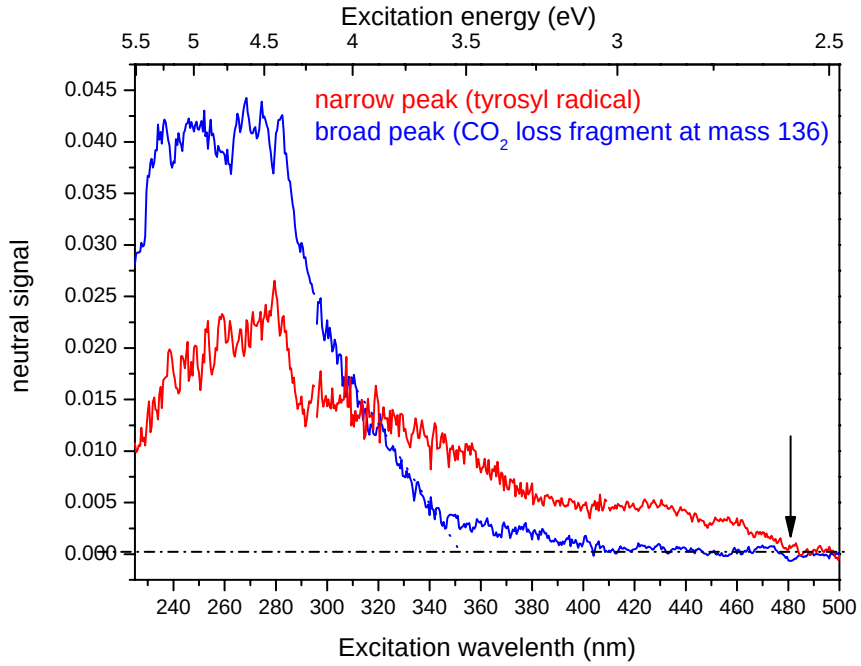

Figure 4. Excitation spectra recorded while scanning the laser with the detection set either on the tyrosyl radical (narrow peak, red trace) or on the fragment at mass 136 (blue trace).

$[Trp\text{-}H]^-$ anion

The TOF mass spectra corresponding to neutrals due to the photodetachment of the anion, either intact tryptophanyl radicals or its fragments, were recorded at different excitation energies (Figure 5). As in the case of $[Tyr\text{-}H]^-$, at low excitation energies (< 3.7 eV), only the intact parent radical is observed as a narrow peak. At higher excitation energies (> 3.7 eV), the mass spectra show three components corresponding to tryptophanyl radicals (narrow peak) and two fragments (broad peaks).

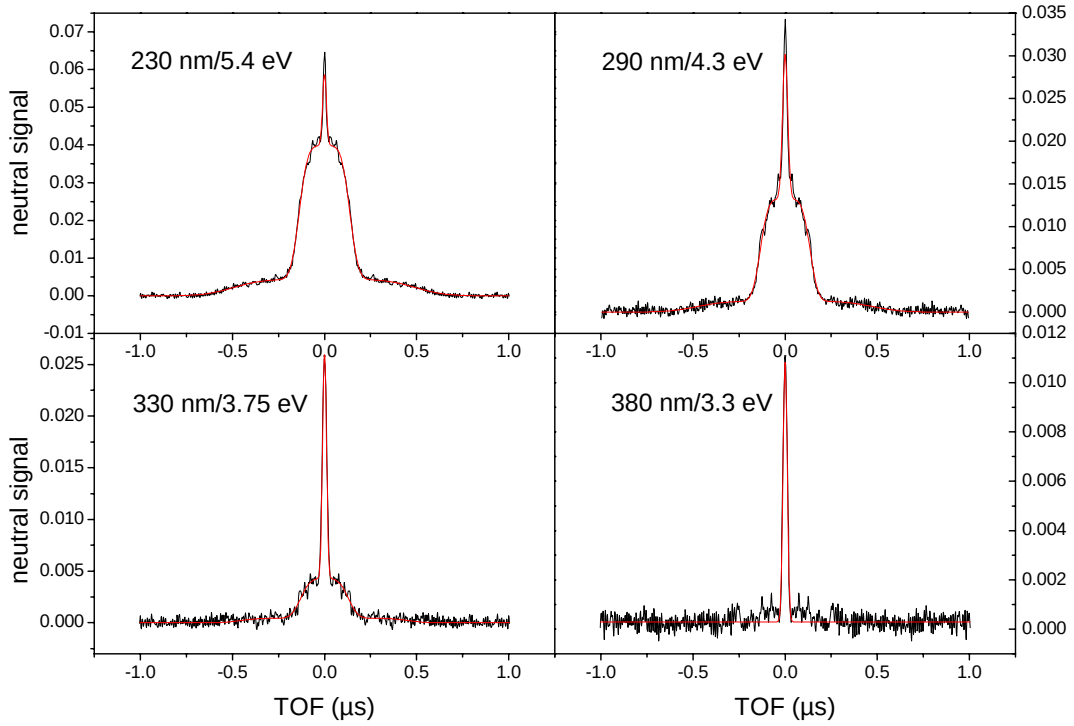

Figure5.Time of Flight peak profiles obtained at different excitation energies for [Trp-H]$^-$. The profiles have been symmetrized and are fitted with a sum of a Gaussian function for the narrow peak (tryptophanyl radical) and two combinations of erf functions of different widths for the wider fragment peaks (see supplementary information for the symmetrization and fitting procedure).

The same fitting procedure as for [Tyr-H]$^\bullet$ and its fragments has been applied to the peak profiles: symmetrization and fitting with two combinations of erf functions for the two fragments and a Gaussian function for the tryptophanyl narrow peak, the width of which is the same as the width of the parent anion peak, i.e. 20 ns. As can be seen in Figure 5, the fragmentation channel yield increases as the excitation energy increases. From the fitting, we extract the mean widths of the two broad peaks (137 ± 15 ns and 465 ± 60 ns), which remain unchanged as a function of the excitation energy. If we assume that the dissociation channel corresponds to CO_2 loss, as for phenylalanyl and tyrosyl, the ratio of the widths of the two broad peaks, 0.29 ± 0.07, reflects the mass ratio of the two neutral fragments CO_2 and $C_{10}H_{11}N_2$,i.e.is 0.27. Considering the widths of the peaks and the geometry of the TOF mass spectrometer, we can extract the kinetic energy released in the dissociation process, which is (0.19±0.02) eV. (See S.I.4)

The photodetachment and fragmentation thresholds were determined by scanning the laser while monitoring the intensity of the narrow and the broad part of the peak profile (Figure 6A). The

photodetachment threshold (Figure 2B) was found at low energy: 2.85 ± 0.03 eV (440 ± 5 nm), while the photofragmentation signal is weak and slowly increasing from 3.35 eV to 3.75 eV, with a more abrupt increase after 3.75 eV (Figure 2A).

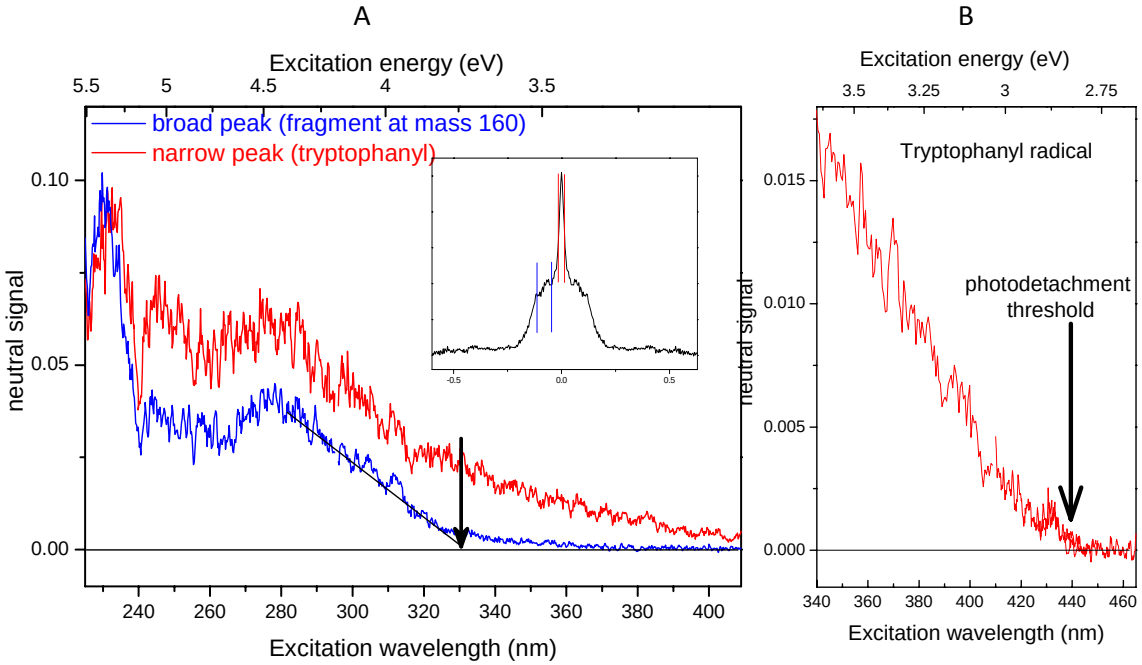

Figure 6.A: excitation spectra recorded by scanning the laser with the detection set either on the tryptophanyl radical (narrow peak, red trace) or on the fragment at mass 160 (blue trace). B: excitation spectrum recorded on the tryptophanyl radical at low energy

c) Calculations

Vertical and adiabatic detachment energies (VDE and ADE) have been calculated for deprotonated aromatic amino acids. In the case of$[Tyr-H]^-$ and $[Trp-H]^-$, two isomers have been considered: one isomer being deprotonated on the carboxylic acid group (labeled $TyrCO_2^-$ or $TrpCO_2^-$) , the other one being deprotonated on the phenolic oxygen or indolic nitrogen ($TyrO^-$ or $TrpN^-$), respectively. The relative energy of the isomers (E_i)is displayed in Table 1.The calculated ADE and VDE corresponds to the most stable conformers previously reported [20].

In all three cases, when the aromatic amino acids are deprotonated on the carbonyl group (RCO_2^-), the radical optimization necessary to obtain the ADE leads to CO_2 loss. The final energy for the CO_2 + R•channel E_{diss} (see Table 1) is referenced to the ground state of the anion and is more than 1 eV below the VDE. In this case, the ADEs shown in Table 1 correspond to calculations in which the C-CO_2 bond distance is maintained at a fixed value while optimizing the other coordinates. Releasing the

constraint after this optimization leads to CO_2 dissociation, indicating the absence of any barrier in the CO_2 loss channel.

Table 1. Vertical and adiabatic detachment energies (VDE and ADE) for deprotonated aromatic amino acids. For deprotonated tyrosine and tryptophan, two isomers have been considered, one isomer being deprotonated on the carboxylic acid group ($TyrCO_2^-$ or $TrpCO_2^-$*), the other deprotonated on the phenolic oxygen or indolic nitrogen (*$TyrO^-$ or $TrpN^-$*), respectively. When the molecules are deprotonated on the carbonyl group, the radical optimization leads to CO_2 loss (the final energy for CO_2 + R• is E_{diss}) and in this case the ADE values correspond to calculations where the C-CO_2 bond is maintained at a fixed value, the other coordinates being optimized. All values are in eV.*

DFT/B3LYP **aug-cc-pVTZ**	**[Phe-H]$^-$ (carboxyl)**	**TyrCO_2^- (carboxyl)**	**TyrO^- (phenol)**	**TrpCO_2^- (carboxyl)**	**TrpN^- (indole)**
E_i	0	0	0.14	0	0.15
VDE	3.65	3.51 3.65[a]	2.54 2.72[a]	3.63	2.79
ADE	3.11	3.11 -	2.39 2.64[a]	3.01	2.56
E_{diss}	2.30[c]	2.32[c]	-	2.56	-
Photodetachment threshold (expt)	3.54 ± 0.02	3.55[b]	2.58 ± 0.03 2.70[b]	-	2.85 ± 0.03
Photofragmentation threshold (expt)	3.54 ± 0.02	3.54	3.10 ± 0.05	3.75 ± 0.05	3.25± 0.05

[a]calculated value from ref.Tian et al [5]

[b] experimental value from ref. Tian et al [5]

[c] referenced to the energy of the ground state of the carbonyl ion

Discussion

[Phe-H]$^-$

The phenylalanine case is the simplest since there is only one possibility for removing a proton from phenylalanine, i.e. from the carboxylic acid group. The [Phe-H]$^-$ion does not photofragment below the photodetachment threshold, and thus we observe only photodetachment. The phenylalanyl radical produced by photodetachment of [Phe-H]$^-$is unstable and loses CO_2 as soon as the photodetachment threshold is reached, at (3.54±0.02) eV, which is slightly lower than the calculated VDE value (3.65 eV) and even lower than the experimental VDE previously reported by other

authors(3.91 ± 0.19 eV)[21].In agreement with the experimental data, the geometry optimization process leads directly to CO_2 loss with a dissociation energy calculated at 2.3 eV above the ground state of the anion, i.e. 1.24 eV lower than the photodetachment threshold.

The widths of the fragment peaks do not vary with the excitation energy, which means that the kinetic energy released in the fragmentation process does not depend on the excitation energy, which in turn means that the excess energy is transferred to the electron. The kinetic energy released in the dissociative photodetachment process can be compared to the impulsive model[22]in which all the atoms except those involved in the chemical bond that breaks are spectators. The kinetic energy release upon CO_2 loss is $E_{kin}= (\mu_{\alpha\beta}/\mu_{AB})*E_{avl}$, where E_{avl} is the available energy, here 1.24 eV, $\mu_{\alpha\beta}$ is the reduced mass of atoms α and β (α–β being the bond that breaks), and μ_{AB} is the reduced mass of the two fragments A and B. In the present case, the calculated kinetic energy is E_{kin}= 0.23 eV, in good agreement with the experimental value of 0.20±0.02 eV.

[Tyr-H]$^-$ and[Trp-H]$^-$

There are two possibilities for removing a proton from tyrosine and tryptophan: either from the carboxylic acid group or from the phenol (OH) or indole (NH) chromophores, which leads to two different isomers for the deprotonated forms of tryptophan and tyrosine (labeled $TyrCO_2^-$ or $TrpCO_2^-$ for deprotonation on the carboxylic acid group and $TyrO^-$ or $TrpN^-$ for deprotonation on the chromophore).

The two isomers of deprotonated tyrosine have already been observed via their photoelectron spectroscopy, the observed ADE and VDE being 3.55 and 3.90 eV for $TyrCO_2^-$ and 2.70 and 2.74 eV for $TyrO^-$.[5]Our action spectrum following the intact parent radical looks very much like this previously reported photoelectron spectrum. The photodetachment threshold observed at (2.58±0.03) eV is assigned to the $TyrO^-$ isomer, in agreement with the calculated VDE value (2.54 eV).In addition, this value is 0.33 eV higher than the photodetachment threshold reported for the phenolate anion (2.2538 eV) [2324].

The action spectrum recorded while detecting the neutral fragments shows a clear and rapid increase of the fragmentation channel at 3.54 eV, which corresponds to fragmentation from the $TyrCO_2^-$ isomer, in agreement with both the photoelectron spectrum reported by Tian et al. and the calculated VDE of 3.51 eV. There is also a weak and slowly increasing fragmentation from 3.1 to 3.54 eV. The origin of this minor fragmentation signal from the $TyrO^-$ isomer is unclear. One possible explanation is that fragmentation is induced by either proton transfer from the acid group to the phenolic oxygen leading to concerted CO_2^- rupture and photodetachment in the ion or by a concerted hydrogen transfer and CO_2 rupture in the radical. Such a signal would only be observed if the excess energy was high enough to allow hydrogen migration.

As in the case of deprotonated phenylalanine, above the fragmentation threshold of the $TyrCO_2^-$ isomer the widths of the fragment peaks do not vary with the excitation energy, which means that the excess energy is transferred to the electron. The dissociation threshold for the CO_2 $+C_8H_{10}NO^\bullet$channel is calculated at 2.32 eV above the anion ground state energy, i.e. 1.22 eV lower than the experimental dissociation threshold for the $TyrCO_2^\bullet$radical(3.54 eV).The experimental kinetic energy release of 0.22 ±0.04 eV compares well with the value obtained via the impulsive model[22]: E_{kin}=0.22 eV.

Deprotonated tryptophan is very similar to deprotonated tyrosine: the photodetachment threshold is observed at 2.85±0.03 eV while the dissociation channel is observed above 3.75 eV, with two broad bands centered at around 4.4 eV and 5.4 eV. It may be noted that, in the 3.80 eV to 5.5 eV energy region, our spectrum is similar to that recorded by Compagnon et al. from depletion of the parent anion[6].However, our photodetachment threshold is lower than their value of 3.94 eV.The photodetachment threshold observed is also quite different from the electron affinity reported in the literature for the [Trp-H] radical(3.90 ± 0.19 eV)[21]. It is likely that these observed differences are due to the different experimental methods used to derive the values. Comparing the experimental thresholds with the calculated VDE for the two isomers of $[Trp-H]^-$ (2.79 eV for $TrpN^-$ and 3.63 eV for $TrpCO_2^-$)as well as to the deprotonated tyrosine case, we assign the photodetachment threshold at 2.85 eV to the $TrpN^-$isomer, and the dissociation threshold at 3.75 eV to the $TrpCO_2^-$ isomer. As in the case of $TyrO^-$ compared to the phenoxide, the photodetachment threshold for the $TrpN^-$ isomer is higher (by 0.42 eV) than the photodetachment energy of the indoline anion.[12]Additionally, as for Tyr, there is a weak fragmentation component observed to increase very slowly from 3.35 to 3.75 eV below the photofragmentation threshold of $TrpCO_2^-$. Once again, a concerted hydrogen/ proton transfer from the acid group to the N may be at play.

As in the other cases, the widths of the fragment peaks do not vary with the excitation energy, indicating that the electron removes all excess energy. The dissociation threshold for the CO_2 $+C_{10}H_{11}N_2^\bullet$channel is calculated at2.56eV above the anion ground state energy, i.e.1.19 eV lower than the experimental dissociation threshold for the $TrpCO_2^\bullet$radical (3.75 eV). The experimental kinetic energy release is 0.19 ±0.02 eV, in agreement with the value obtained via the impulsive model: E_{kin}=0.20 eV.

Conclusion

When aromatic amino acids are deprotonated on the carbonyl group, the radicals produced upon photodetachment dissociate without barrier, leading to the formation of CO2 and a radical amine. This is in contrast to our previous results for benzoate and naphthoate, where barriers to CO2 loss were observed. When the system is deprotonated on functional groups located on the chromophore (OH for Tyr or NH for Trp), the radicals produced by photodetachment are stable. The role of the amino acid group on the electron binding energy of the chromophore is quite significant, since it increases the photodetachment threshold by more than 15%compared to the neat chromophores phenol and indole. In no case could ionic dissociation be evidenced, probably because the ionic excited states are higher in energy than the ADE.

Conflicts of interest

There are no conflicts to declare.

Acknowledgments

This work has been conducted within the International Associated Laboratory LEMIR (CNRS/CONICET) and was supported by CONICET, FONCyT, SeCyT-UNC and the ANR Research Grant (ANR2010BLANC040501-ESPEM and ANR17CE05000502-Wsplit). We also acknowledge the use of the computing facility cluster Meso-LUM of the LUMAT federation (LUMAT FR 2764).

Supplementary information

1) Experimental setup for the study of anions and neutrals
2) Symmetrization of the mass peaks
3) Neutral fragment peak analysis
4) Kinetic energy released in the fragmentation process.
5) Xyz coordinates of the geometries of deprotonated anion or radical calculated at the DFT/B3LYP/aug-cc-pVTZ level

References

1 R. E. Continetti and H. Guo, *Chem. Soc. Rev.*, 2017, **46**, 7650–7667.

2 Y. Z. Zhou, S. Li, Q. S. Li and S. W. Zhang, *J. Mol. Struct. THEOCHEM*, 2008, **854**, 40–45.

3 J. Oomens, J. D. Steill and B. Redlich, *J. Am. Chem. Soc.*, 2009, **131**, 4310–4319.

4 H. Li, Z. Lin and Y. Luo, *Chem. Phys. Lett.*, 2014, **598**, 86–90.

5 Z. Tian, X. Bin Wang, L. S. Wang and S. R. Kass, *J. Am. Chem. Soc.*, 2009, **131**, 1174–1181.

6 I. Compagnon, A.-R. Allouche, F. Bertorelle, R. Antoine and P. Dugourd, *Phys. Chem. Chem. Phys.*, 2010, **12**, 3334–3335.

7 D. Schröder, M. Buděšínský and J. Roithová, *J. Am. Chem. Soc.*, 2012, **134**, 15897–905.

8 H. Xia and A. B. Attygalle, *Anal. Chem.*, 2016, **88**, 6035–6043.

9 L. Feketeová, G. N. Khairallah, R. A. J. O'Hair and S. B. Nielsen, *Rapid Commun. Mass Spectrom.*, 2015, **29**, 1395–1402.

10 J. H. Bowie, *Mass Spectrom. Rev.*, 1979, **9**, 349–379.

11 G. A. Pino, R. A. Jara-Toro, J. P. Aranguren-Abrate, C. Dedonder-Lardeux and C. Jouvet, *Phys. Chem. Chem. Phys.*, 2019, **21**, 1797–1804.

12 D. J. Nelson, A. M. Oliveira and W. C. Lineberger, *J. Chem. Phys.*, 2018, **148**, 1–8.

13 I. Alata, J. Bert, M. Broquier, C. Dedonder, G. Feraud, G. Grégoire, S. Soorkia, E. Marceca and C. Jouvet, *J. Phys. Chem. A*, 2013, **117**, 4420–7.

14 G. Féraud, C. Dedonder, C. Jouvet, Y. Inokuchi, T. Haino, R. Sekiya and T. Ebata, *J. Phys. Chem. Lett.*, 2014, **5**, 1236–1240.

15 M. Berdakin, G. Féraud, C. Dedonder-Lardeux, C. Jouvet and G. A. Pino, *Phys. Chem. Chem. Phys.*, 2014, **16**, 10643–10650.

16 W. C. Wiley and I. . McLaren, *Rev. Sci. Instrum.*, 1955, **26**, 1150.

17 M. Barat, J. C. Brenot, J. A. Fayeton and Y. J. Picard, *Rev. Sci. Instrum.*, 2000, **71**, 2050.

18 *a Dev. Univ. Karlsruhe Forschungazentrum Karlsruhe GmbH, 1989-2007, Turbomole GmbH, since 2007; available from http//www.turbomole.com Dev. Univ. Karlsruhe Forschungszentrum Karlsruhe GmbH, 1989-2007, TURBO*.

19 D. E. . Woon and T. H. Dunning Jr., *J. Chem. Phys.*, 1993, **98**, 1358.

20 U. Purushotham and G. N. Sastry, *J. Comput. Chem.*, 2014, **35**, 595–610.

21 R. A. J. O'Hair, J. H. Bowie and S. Gronert, *Int. J. Mass Spectrom. Ion Process.*, 1992, **117**, 23–36.

22 Z. Lu and R. E. Continetti, *J. Phys. Chem. A*, 2004, **108**, 9962–9969.

23 S. J. Kregel and E. Garand, *J. Chem. Phys.*, 2018, **149**, 0–9.

24 J. B. Kim, T. I. Yacovitch, C. Hock and D. M. Neumark, *Phys. Chem. Chem. Phys.*, 2011, **13**, 17378–17383.

Supplementary information

Experimental setup for the study of anions and neutrals

1 Dissociation in the trap: ionic fragmentation

2 Excitation after the acceleration in the gauss tube: detection of neutral

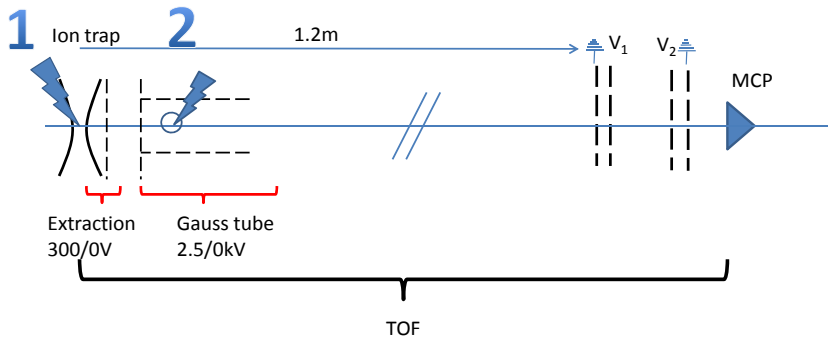

Figure SI-1: Scheme of the experimental setup. The two regions where the laser interacts with the ion packet are 1) in the cold trap, and 2) in the gauss tube.

Symmetrization of the mass peaks

As can be seen in Figure SI-2 panel A, the raw data anion signal, as well as the neutral signal,is not symmetrical, but broadened towards higher times of flight due to electronic ringing in the detector…. One way to get rid of this deformation is to subtract a baseline, as in panel B, but we have to estimate the baseline, and the resulting fit is not optimal. Another method is to take the first half of the signal (up to the peak maximum), reverse it, and add the two components, as illustrated in panel C. We then obtain a good fit with a three component function: a Gaussian function for the narrow peak -C*exp(-(x^2/l^2))- and two combinations of erf functions for the fragments A*((1-erf((x-w)/l1))+(1-erf((-x-w)/l1)))-2*A where w represents the half width at half maximum of the function(see panel D).

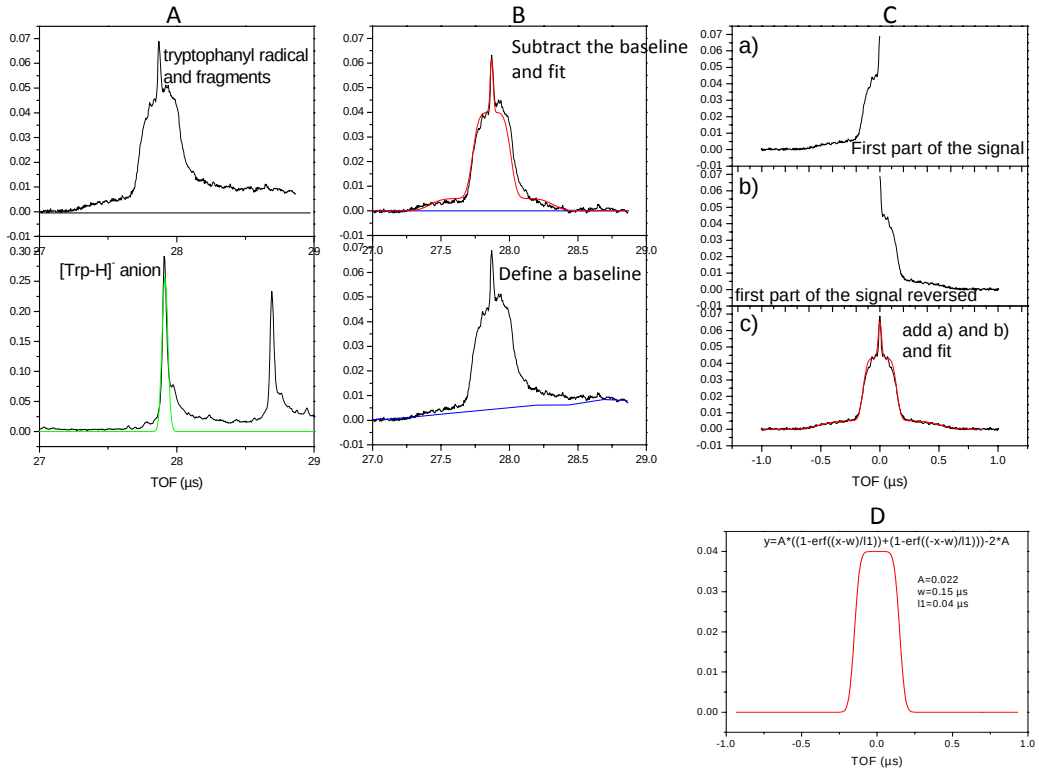

Figure SI-2: panel A,raw time of flight mass spectra as recorded with the MCP detector. Panel B, subtraction of a baseline and fit. Panel C, symmetrization by selecting the first half of the peak, reversing it, and adding the two contributions. Panel D, combination of erf functions to fit the fragment profile of the form A((1-erf((x-w)/l1))+(1-erf((-x-w)/l1)))-2*A, where w represents the half width at half maximum of the function, l1 the slope of the erf functions.*

Neutral fragment peak analysis

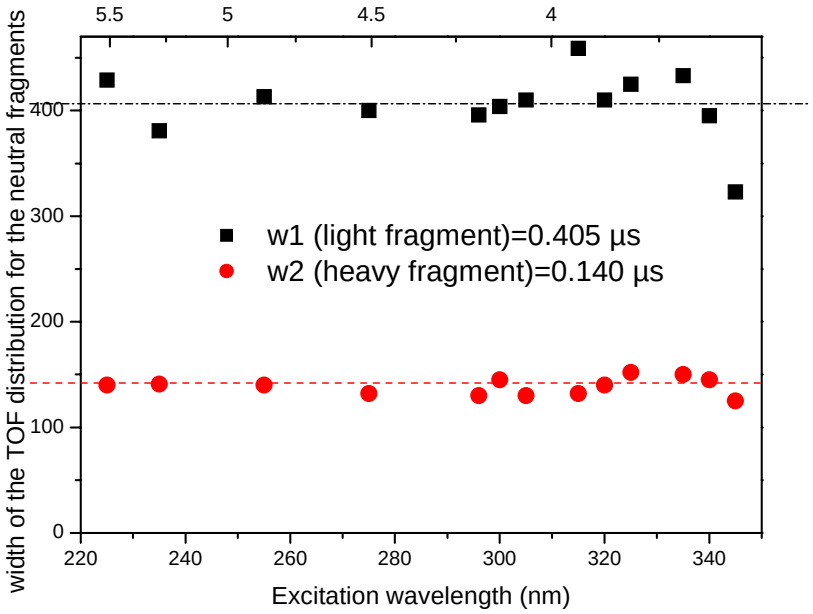

Figure SI-3. Variation of the widths of the fragment peaks as a function of the excitation wavelength for the fragments of the [Phe-H]• radical

Figure SI-4.Kinetic energy released in the fragmentation process.

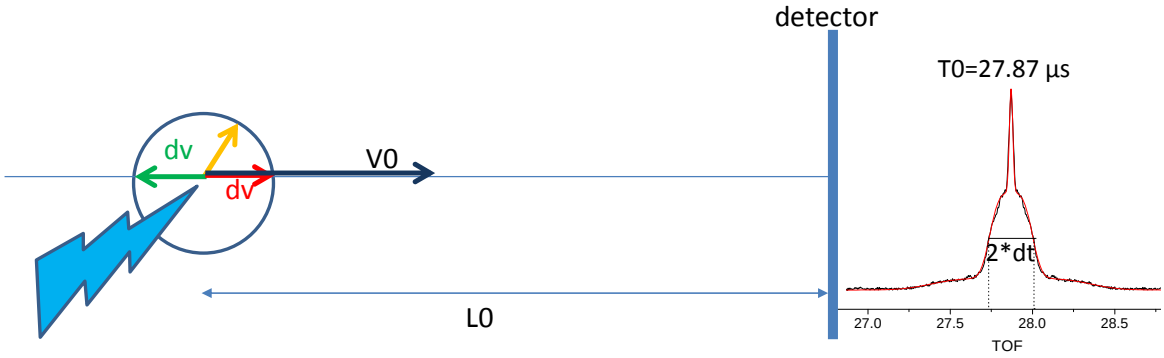

A parent ion with a velocity V0 will arrive at the detectot at time T0= L0/V0
a fragment ion has the initial velocity of the parent plus a relative velocity dv due to the fragmentation process (we assume here that dv is the maximum velocity that can be imparted to the fragment).
If dv is in the opposite direction to V0, the fragment will arrive later on the detector at time T0+dt.
Conversely, if dv is in the same direction as V0, the fragment will arrive sooner on the detector at time T0-dt
and all the fragments that have an initial velocity in another direction or a smaller velocity will arrive at a time between T0-dt and T+dt.

V0=L0/T0, V0-dv=L0/(T0+dt)…. V0-dv=V0(1-dt/T0+(dt/T0)^2-…), dt/T0 is small (0.13/27.87)
Then dv=V0*dt/T0 and the relative kinetic energy of fragment m_f is

$$E_{kin}=1/2*m_f*(V0*dt/T0)^2=1/2*m_f*(L0/T0)^2*(dt/TO)^2$$

Geometries of deprotonated anion or radical calculated at the DFT/B3LYP/aug-cc-pVTZ level

Phenyl alanine aniondeprotonated on CO_2

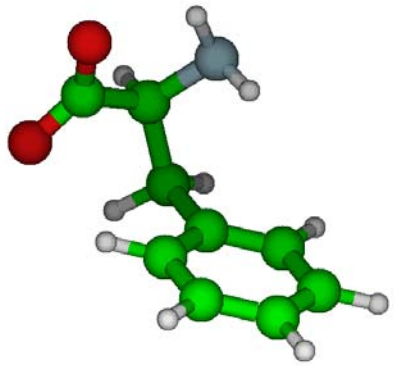

1 c	0.16865091238731	-0.25415226304652	0.25836602724172
2 c	0.41456381453982	0.44948970492088	2.77697528026225
3 c	2.77341038704134	1.12384844586595	3.73025864917984
4 c	4.92861196611267	1.11035955441249	2.20486114397444
5 c	4.65127661420242	0.40601932015652	-0.33256682744145
6 c	2.30000824331672	-0.26811573800071	-1.28720507391389
7 c	7.48587253491187	1.82319214183266	3.25676844904883
8 c	8.49911402170535	4.42170690584230	2.43469350491675
9 c	9.26969693423235	4.54676326724159	-0.44218629418933
10 o	8.87143439177082	6.62351148122967	-1.50607463908593
11 h	-1.66101964217337	-0.77927078938879	-0.49495765025628
12 n	6.81291789894409	6.48639144721865	3.23425380352489
13 o	10.28177356520158	2.59408846802207	-1.32753846628611
14 h	7.17621789691949	7.89780862023176	1.97332836587437
15 h	10.29216824961529	4.66558853561591	3.44649923495727
16 h	7.38566556141583	1.77473789097372	5.32106167240502
17 h	8.88102956512812	0.43863980138080	2.64228774645031
18 h	2.95054261065437	1.67276057903125	5.69550911234131
19 h	6.30954703507718	0.43089801321741	-1.53161826116454
20 h	-1.22553576260103	0.47980879904034	4.00229088004463

Radical –C---CO2 fixed

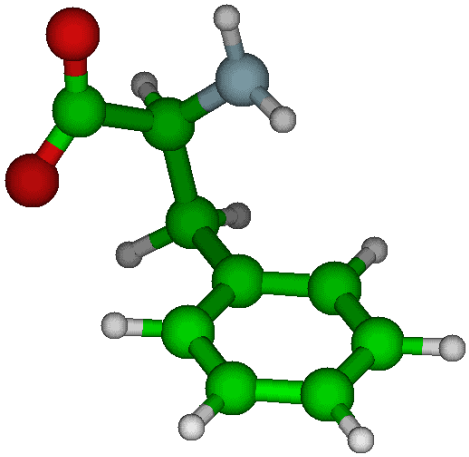

1 c	-6.09090851359800	1.13531954023667	-1.15321827777162
2 c	-5.63380416686941	0.77801489778018	1.40723064735399
3 c	-3.39485552174641	-0.35359782194246	2.19636125248942
4 c	-1.57504461066894	-1.13851978013159	0.44943495917408
5 c	-2.06457006619120	-0.77658704539202	-2.12097317990815
6 c	-4.30110847242929	0.34912371486595	-2.91155708150178
7 c	0.85138164149856	-2.35969605630578	1.34169041202110
8 c	3.11120632514979	-0.56379940929722	1.65592232198492
9 c	4.61101367896291	0.23899742838096	-0.80067137639047
10 o	6.12172172285127	1.94494896331005	-0.45028315947106
11 h	-7.83260254817667	2.00587086150096	-1.77592873527155
12 n	2.50389367912626	1.59391781888687	3.05819975706147
13 o	3.99968591170458	-1.13399226845655	-2.58530151434563
14 h	3.88380164413895	2.91482422992733	3.12705899053461
15 h	4.66713231467567	-1.58797575177256	2.56466815166193
16 h	0.52466940034622	-3.21450301676702	3.19118047753538
17 h	1.41684963166303	-3.85756469042205	0.05549438205285
18 h	-3.07302581920985	-0.66151867356052	4.19514620385332
19 h	-0.68072764848504	-1.37866504556755	-3.49746223408055
20 h	-7.02030086364945	1.36239723196606	2.79183297776067
21 h	-4.65007653962269	0.60609274999538	-4.90984586388169
22 h	0.75284248928950	2.31000809561610	2.78252285105043

C—CO2 free

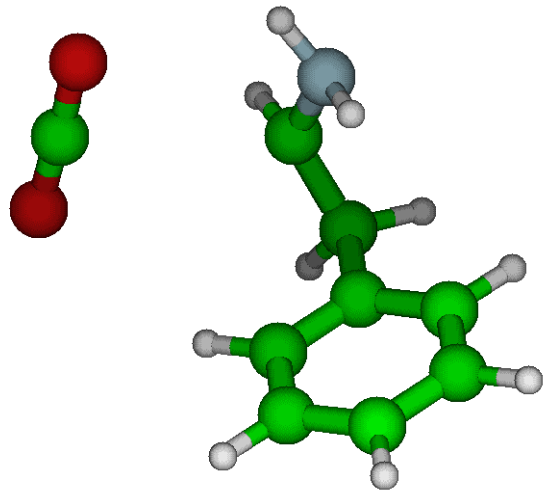

1 c	0.16507534806649	-0.27078463554534	0.21620924081983
2 c	0.19808929064045	0.41330280214110	2.74971363231662
3 c	2.47518830009742	1.01793674400981	3.92425950124909
4 c	4.74798331945495	0.95317485911092	2.59242919206221
5 c	4.68625692837021	0.27466157388837	0.04045143972224
6 c	2.42160649610651	-0.33745048620181	-1.13608297819163
7 c	7.22803514155176	1.62933408864816	3.86415275256727
8 c	8.26877673604632	4.14522734327818	3.09285016458237
9 c	10.12114916478683	5.33090462235400	-2.70353038062186
10 o	9.67054634389591	7.42624855996841	-2.22698137932822
11 h	-1.59828859428247	-0.75217382121331	-0.69931189334066
12 n	6.74375897638459	6.27065773202729	3.37495352712117
13 o	10.60356753368445	3.26212441389759	-3.24980339724940
14 h	7.42060722029110	7.86391774731968	2.57720304223297
15 h	10.27233730638100	4.48463401618785	3.33017575312724
16 h	6.94301671610752	1.55546866677763	5.92339433502590
17 h	8.64094139730366	0.19161564514120	3.42671884368730
18 h	2.48760638724749	1.53289180233159	5.90527559572578
19 h	6.43074493035817	0.22129047147828	-1.02682367303239
20 h	-1.54340701778198	0.47123004332727	3.81983089512267
21 h	2.41624092992967	-0.87528170328793	-3.10900579834480
22 h	4.90050424097583	6.00578255094250	2.95087289530649

Tyrosine anion deprotonated on phenoxy

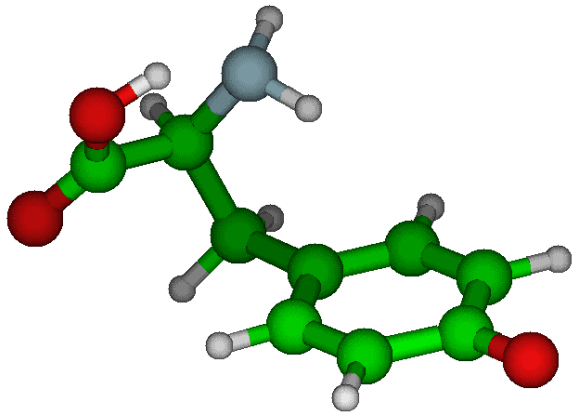

1 n	0.08731893607592	-0.25244351356949	-0.12203400028704
2 h	-0.15038092767218	0.94065427711042	1.37199782360100
3 c	2.73887415133195	-0.10833062897929	-0.95170642267331
4 h	2.79815835536698	-0.13874521613986	-3.01674106579478
5 c	4.12334012769014	-2.54893195194012	-0.18224548456307
6 o	6.32392124735807	-2.94377724033993	-0.63127003499251
7 c	4.14030760869025	2.31946946684994	-0.02904325539235
8 h	3.69819058575667	3.81919084271027	-1.38016765767281
9 h	6.16270261801547	1.94184986607070	-0.19176800005810
10 c	3.41846153315479	3.18322706025511	2.58217318756225
11 c	1.61319062914294	5.09738025555072	2.94480392965426
12 h	0.81279115706252	6.01934719956391	1.28846470210290
13 c	4.43350799709272	2.09133843757311	4.78311090559494
14 h	5.85445819548094	0.62001768896691	4.59654065102123
15 c	0.84033501177501	5.87729399312862	5.31641028722067
16 h	-0.54282292537020	7.37633114879438	5.51499434272217
17 c	3.69497923922455	2.83473244783240	7.17236084721973
18 h	4.52730883738272	1.95929226997194	8.82775578913408
19 c	1.82772928581537	4.78024903389330	7.60930188260323
20 o	1.13892950667281	5.46474474833142	9.79106026544944
21 o	2.63589452769747	-4.25673137713968	0.94816089675463
22 h	0.96793665248393	-3.41383541792348	1.01026617334631
23 h	-1.11820661652626	0.28780002411562	-1.50074840174992

Tyrosine rad dep onPhenyl

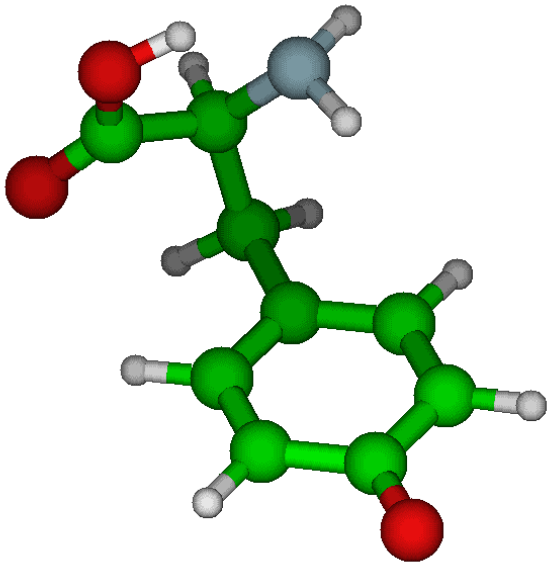

1 n	-2.34470016461140	2.82955649575025	-3.21555965734288
2 h	-2.76913058401107	2.69111512163324	-1.35351916718856
3 c	0.08121694190611	1.63527920292872	-3.81544714334473
4 h	0.81939483004206	2.56406827240692	-5.50542343612384
5 c	-0.34722499160123	-1.11783597195172	-4.65429905057539
6 o	1.34319504875821	-2.61972996561951	-4.88645660712412
7 c	2.16662580144788	1.82841119156115	-1.76703502044393
8 h	2.73141486069690	3.80641901848040	-1.63235659169408
9 h	3.78345841130886	0.75385561375231	-2.45424114559107
10 c	1.38620005546631	0.88690206505149	0.79878919931263
11 c	0.49637266236483	2.59413655620627	2.64624565752756
12 h	0.45837300151722	4.59385035503084	2.20649164579325
13 c	1.50001696220605	-1.71528699422705	1.39761931106822
14 h	2.19840169985107	-3.02003997156457	-0.01289294215441
15 c	-0.28058997269830	1.77742707179292	4.97959692830472
16 h	-0.95929895597406	3.07397962767947	6.40628691216150
17 c	0.74077549221170	-2.58587182442128	3.71356426928432
18 h	0.82343857018192	-4.57155867561253	4.19092881489361
19 c	-0.20665615712536	-0.87882241023186	5.63105241180275
20 o	-0.91765771567179	-1.65292236611434	7.74924818062116
21 o	-2.75279268186007	-1.66859737195631	-5.18998879434182
22 h	-3.71501819818809	-0.12972803128822	-4.80386701253443
23 h	-2.38677697787618	4.67639085244690	-3.69813719655978

Tyrosine deprotonated on CO2

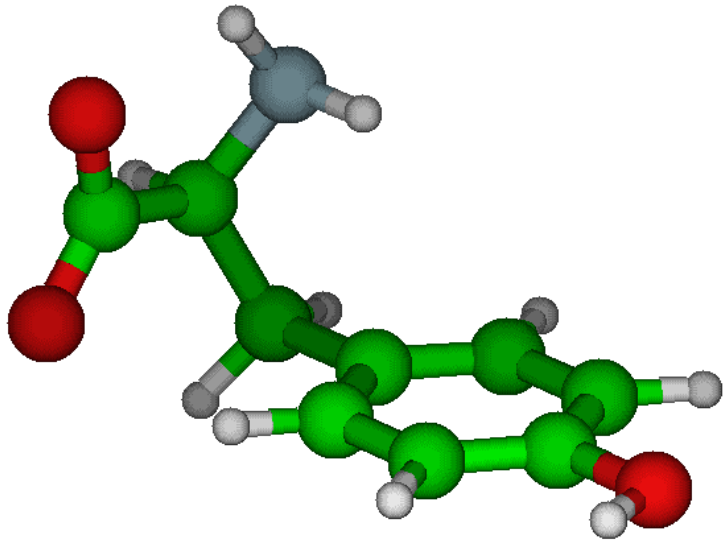

Anion.

1 n	0.19109204607645	-0.29564895266318	0.24242006035000
2 h	0.29223166938765	0.23861161365828	2.09130489822343
3 c	2.79507994085767	0.00548904675671	-0.69304406881894
4 h	3.76421032396840	-1.80668612366649	-0.41861931681936
5 c	4.41869261276810	1.94553666102485	0.88272378766078
6 o	6.47812685186440	2.60013363346470	-0.09526650207409
7 c	2.85790076271253	0.50541113732678	-3.55577679399181
8 h	1.99523542371758	-1.10247542946640	-4.52826641248435
9 h	4.84552691848086	0.58692260157164	-4.08780687653902
10 c	1.55247361657096	2.89726045097223	-4.41521443280041
11 c	-0.74557684390784	2.82840799409098	-5.70920956881890
12 h	-1.61417892902189	1.01416927656517	-6.09536903590285
13 c	2.61520087172863	5.27346254906997	-3.94347240494668
14 h	4.37947378114326	5.36282383931686	-2.90954135505346
15 c	-1.96021880511330	5.01813487542496	-6.52063846129266
16 h	-3.74295826426822	4.93387029675707	-7.51903076013455
17 c	1.42244414176583	7.47136656667652	-4.73981416086121
18 h	2.27378929612468	9.29522775322143	-4.34206715651789
19 c	-0.86600166603745	7.34949568308305	-6.03021972882701
20 o	-2.11105515543351	9.49279370994813	-6.85582953310133
21 o	3.51611127270609	2.56018875003720	2.98272022074423
22 h	-0.89812420192583	1.06091134846790	-0.57039353411658
23 h	-1.15743366442383	10.94733439432629	-6.32802874293679

Radical CC fixed

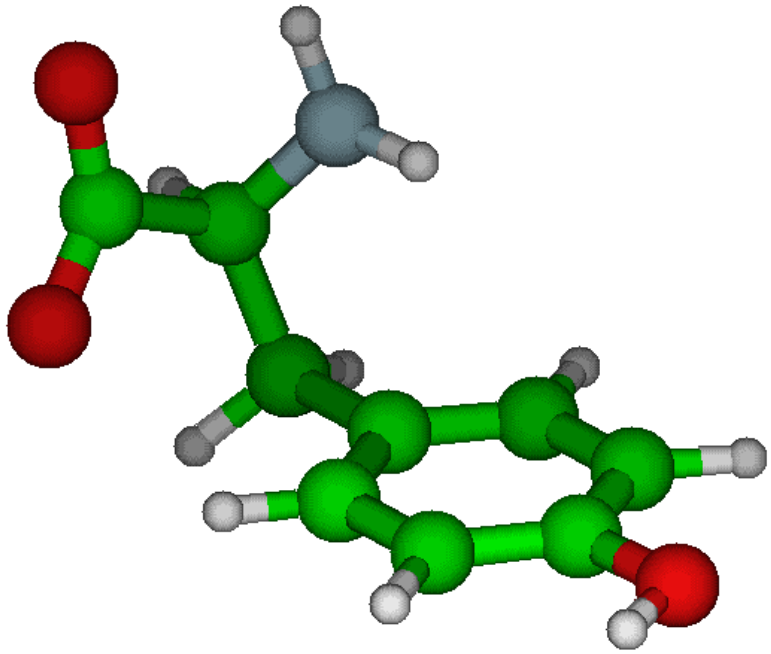

1 n	-2.05703875414633	-2.74433307978794	3.38752064016210
2 h	-3.47893494548639	-2.50709262471879	4.64251416010559
3 c	0.21312061587459	-1.56325869045659	4.05717708813992
4 h	0.98370750500431	-2.42981743534226	5.77524826415005
5 c	-0.36879414145779	1.11308897211048	5.23396987209609
6 o	1.27836535815085	2.64033260033877	4.59868992937803
7 c	2.19956259111908	-1.70063456532078	1.94309230784686
8 h	2.81372366695957	-3.66800836206979	1.84605486620815
9 h	3.81477923357503	-0.57672247698294	2.53352758184692
10 c	1.29801091435380	-0.88603443471875	-0.64296411748194
11 c	0.42894585434069	-2.66751992327122	-2.39071598030860
12 h	0.44347934171269	-4.65439869946006	-1.89508776686574
13 c	1.31066443930996	1.65003979753913	-1.37664722207197
14 h	1.97826414858712	3.06998874232331	-0.06931096368783
15 c	-0.42086076375135	-1.96648246409955	-4.77214379043153
16 h	-1.07956491046827	-3.35992560953260	-6.11312113575636
17 c	0.47028819423504	2.37715645979324	-3.75250876748621
18 h	0.50143293144303	4.35523881452449	-4.28433953432164
19 c	-0.40555234076097	0.57172841636778	-5.45740307497798
20 o	-1.25299889385378	1.17984665544212	-7.81882746580018
21 o	-2.22882610135704	1.14586479964090	6.59744087373616
22 h	-2.58893307848929	-2.55619477688455	1.56062977555740
23 h	-1.14550174058174	2.97833644273237	-8.06973518650852

Radical Without constrain on the CC bond after 30 step of optimization

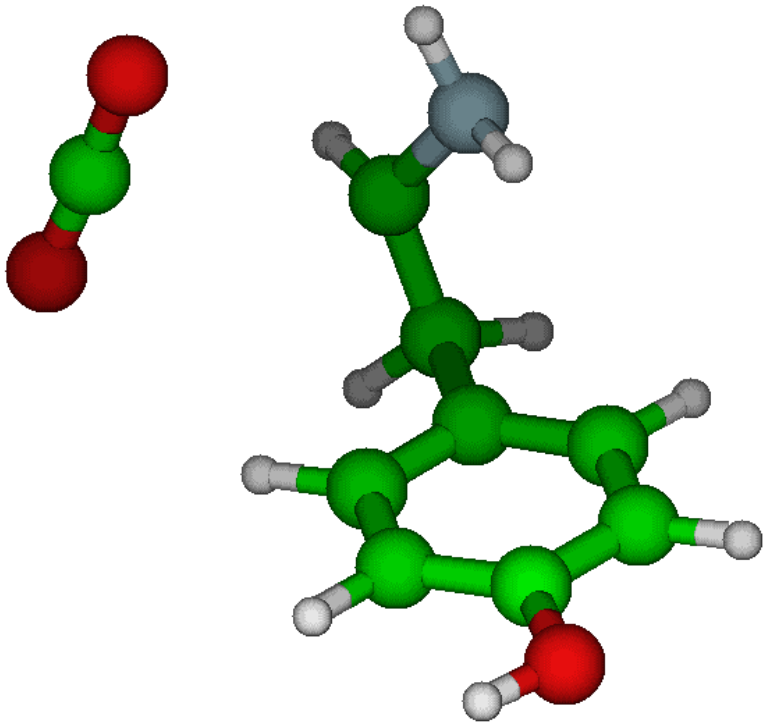

1 n	0.04093495372257	-0.37395502325248	-0.11531545310275
2 h	0.02902241470023	-0.55582469774193	1.78196509187458
3 c	2.41885679827831	-0.36110634498989	-1.23951066032412
4 h	3.74518546449896	-1.71106262230362	-0.45982770019786
5 c	5.60779579336056	3.09498575369787	2.59353018954085
6 o	7.21117763142793	3.49517691180830	1.14961821588335
7 c	2.60730453337436	0.26780888300662	-3.99372554106203
8 h	1.74078795369488	-1.23537988032806	-5.14271124767680
9 h	4.60509272229448	0.29954666180165	-4.50582356237349
10 c	1.38695996054502	2.75881281586243	-4.71528844493003
11 c	-0.98355671547782	2.84515331902129	-5.86716116456968
12 h	-1.95666662371836	1.09407709829207	-6.28926155673692
13 c	2.59593610492285	5.05185317652094	-4.22714819277896
14 h	4.43980411773682	5.04865284369952	-3.34030643652916
15 c	-2.12615510423825	5.12211339483309	-6.50813567653795
16 h	-3.96164098104702	5.16900093817100	-7.40492460015937
17 c	1.48752872329718	7.34269415583679	-4.86739399958062
18 h	2.47186086814726	9.09992764618434	-4.49074510498900
19 c	-0.88522070480108	7.38287382258471	-6.00866459316969
20 o	-2.07437253141718	9.58253072386885	-6.67484987736033
21 o	4.05468545774235	2.74171152837617	4.10407745408026
22 h	-1.13148045871467	1.02075701715046	-0.68965366143361
23 h	-1.02179459913585	11.00239544359054	-6.24718146719995

TRP anion deprotonated on CO2

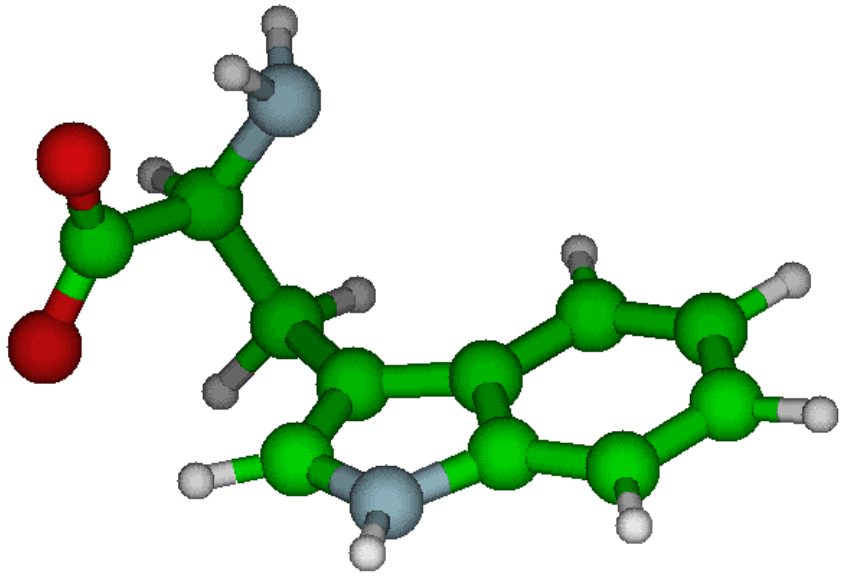

1 n	0.52768610527851	-1.19355049942161	-0.06924010476488
2 h	0.91641871424601	-2.04873592675984	1.61494450056308
3 c	2.98873411503976	-0.27049785513588	-0.97332753753218
4 h	3.56862055192035	-1.30466994579041	-2.67371324642338
5 c	5.14546804414503	-0.77495686950151	1.01645593178419
6 o	4.55117190506973	-2.10348202325628	2.88417900730597
7 c	2.88554205897985	2.54531281466465	-1.73939509108134
8 h	4.69619516738275	2.99822059415026	-2.61622153093111
9 h	1.42096326234976	2.77524867020388	-3.17900251486940
10 c	2.38497954859575	4.35841534939567	0.38749342274723
11 c	3.94621162866067	4.81291351553098	2.39721004498649
12 h	5.73701887065005	3.93896059136119	2.81794018221910
13 c	0.21532234793748	5.95766413598184	0.74458478196846
14 n	2.88282785428328	6.60614239254147	3.97814282862802
15 h	3.61440309588853	7.15349554227851	5.63738500041925
16 c	0.58689255897863	7.34049733298298	3.02157625278755
17 c	-2.01570460558809	6.36921268222554	-0.62103542438360
18 h	-2.37034156272606	5.32738246002502	-2.34473822730669
19 c	-1.17910233314498	9.07172704825381	3.92401313126157
20 h	-0.86422116690819	10.09969335460260	5.66717327740275
21 c	-3.77592479867278	8.09340497283245	0.26749528832563
22 h	-5.50562732931782	8.40758696733402	-0.78040651028961
23 c	-3.36504313789008	9.43545236338114	2.52231476011997
24 h	-4.77525053700531	10.76471190906054	3.17851439880090
25 o	7.23822738315491	0.21683234409946	0.51563881189657
26 h	-0.14802828955308	-2.55056942777157	-1.23506607202346

Radical

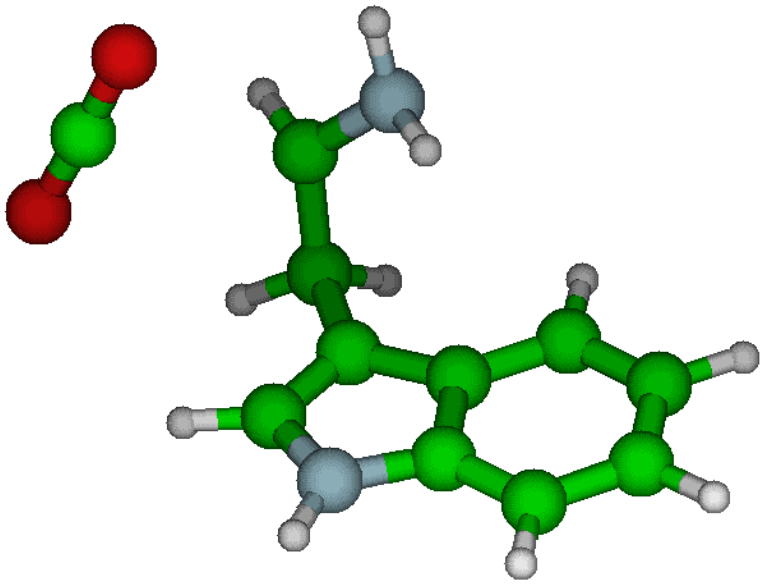

1 n	-4.06556346565252	-2.63977960970772	1.15341218768968
2 h	-3.19520318189824	-1.12283663498732	1.94400408167724
3 c	-2.76868940459854	-3.75091138491116	-0.86231006550992
4 h	-3.60726229589053	-5.50645970163668	-1.55274845779715
5 c	1.53860824549740	-7.20610002022106	1.61718073935416
6 o	0.27548378485659	-7.34514619716112	3.42274183691075
7 c	-1.51727086177122	-2.04508022775211	-2.76985294059102
8 h	-0.43585187774907	-3.24196820466873	-4.07806211853112
9 h	-2.96225730967751	-1.07394658417539	-3.94060857905076
10 c	0.21257264830673	-0.06572187335156	-1.66122215373202
11 c	2.78995458297811	-0.26383425669578	-1.36849482035894
12 h	4.04067730637719	-1.81305911361585	-1.86224543709999
13 c	-0.47525974721533	2.40184966565661	-0.70353358788974
14 n	3.74243839438288	1.92000846770549	-0.28306817263797
15 h	5.58148975946991	2.24704352356353	0.09171313971783
16 c	1.78775702518153	3.59453531091486	0.14206999840834
17 c	-2.77703336864379	3.73235646021349	-0.50184731366333
18 h	-4.54165286543969	2.87324679241408	-1.12890206172359
19 c	1.80687029578146	6.03445224014749	1.17182746086466
20 h	3.55621319960811	6.92092617820954	1.80626210231110
21 c	-2.76649523781500	6.15747092800691	0.51824779747366
22 h	-4.53513006712033	7.20272709859845	0.68108629719110
23 c	-0.49739084925814	7.29739066954193	1.34874449957369
24 h	-0.54933488413149	9.19956448264943	2.14016078121323
25 o	2.87994593865503	-7.14083581638826	-0.13690164653521
26 h	-4.69630015194929	-3.85708249202693	2.48954042361946

Radical CC-fixed

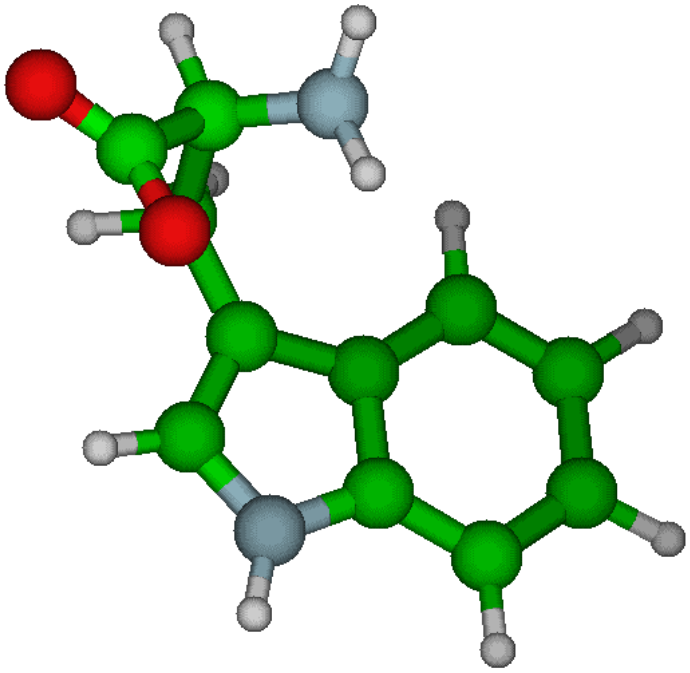

1 n	-3.58842970896621	-2.74249664435268	1.35811565870386
2 h	-2.44539440061223	-1.85529098003560	2.60953582251437
3 c	-2.29254611192938	-4.05476174639724	-0.55577480682781
4 h	-3.61322059308870	-5.24691821588126	-1.57436658373128
5 c	-0.17154237913709	-5.80954012327845	0.57549754554472
6 o	1.18254291895562	-4.80607031372513	2.16190080645818
7 c	-0.92829031857737	-2.30575540687949	-2.51885482397093
8 h	0.21430717987383	-3.52896798274878	-3.71702918123189
9 h	-2.45255891396254	-1.55681749044022	-3.69357717478170
10 c	0.59773375512295	-0.19098416209867	-1.48434355210613
11 c	3.17609202912268	-0.16865308855296	-1.16514666940217
12 h	4.52671740138320	-1.64357814139366	-1.54029862760306
13 c	-0.29470784348326	2.23165663468269	-0.62010487654204
14 n	3.93018064627486	2.09477729015143	-0.16918718089928
15 h	5.71877862539254	2.54827742251113	0.27211175950195
16 c	1.84489997418823	3.61963072656770	0.19599887048805
17 c	-2.68170459780957	3.36732845701551	-0.46644726983835
18 h	-4.35273969359930	2.35896751764944	-1.07230336851011
19 c	1.66422492293332	6.06329257596236	1.14716379410727
20 h	3.31864770801493	7.09723043732196	1.76166601448458
21 c	-2.87261125382053	5.79949522705204	0.48442563446587
22 h	-4.70622650829633	6.69387643875188	0.61358892777636
23 c	-0.72464230239234	7.13356283235478	1.28294422315113
24 h	-0.93404283804720	9.03055819896934	2.01399884496711
25 o	-0.30409240667403	-7.91289683843504	-0.44083128325068
26 h	-4.99006107812565	-3.70711619557046	2.2185099324286

Anion deprotonated on indole

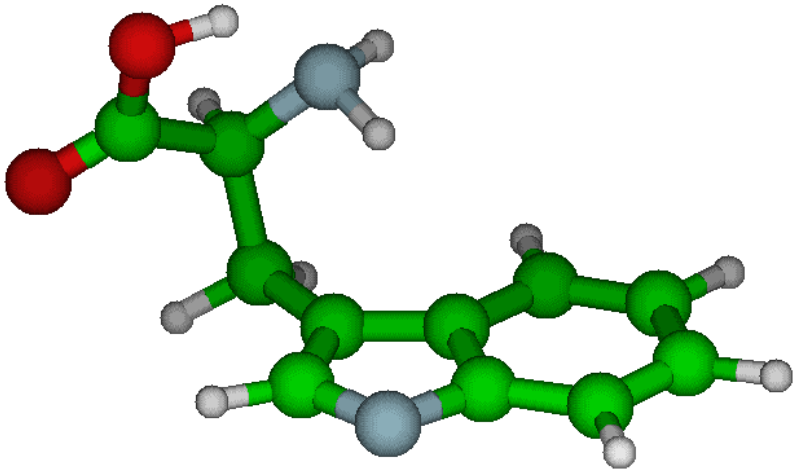

1 c	-0.07941896584551	0.52590159833412	-0.22265335494369
2 c	-0.08941086880027	0.37973245035178	2.39542639791044
3 c	2.19260286484681	0.01163667105852	3.68831520099709
4 c	4.52467396078646	-0.22262087246027	2.28688977900201
5 c	4.47930315488693	-0.05476125545532	-0.36529773833003
6 c	2.19434517703601	0.31665800738041	-1.59674426468076
7 n	2.59941748445347	-0.16516624853155	6.22788333182100
8 c	5.11835188306881	-0.50717935022860	6.45818438410848
9 c	6.43399444809020	-0.56725732240663	4.15561491145816
10 c	9.20272315274548	-0.93982191018166	3.72044664224005
11 c	10.02754776421784	-3.75683469299002	3.46132530039619
12 c	10.63141921002831	-4.96953794350959	6.03661853850604
13 o	12.03947231520036	-4.04443526819702	7.57314363871864
14 n	8.18757384259374	-5.35466611041025	2.11648728645525
15 o	9.52963897438716	-7.22285410510592	6.38278302996619
16 h	8.54465299380642	-7.47005756531810	4.81008617075896
17 h	11.82654130482936	-3.82244741807580	2.44658957323946
18 h	10.33078462945607	-0.11740383616996	5.23951049522276
19 h	9.76622826215042	0.02132950561312	1.97674415889866
20 h	5.96298694096284	-0.69744109633055	8.31613150544534
21 h	6.20934661781077	-0.19691816989463	-1.46224183968230
22 h	-1.83596549817119	0.55171634372428	3.45337801762145
23 h	2.15092543241407	0.45275678333189	-3.64088455493205
24 h	-1.83877608084616	0.80826449078692	-1.23366663295184
25 h	8.61379514509236	-5.50150994294147	0.26050953297007
26 h	6.46180989902599	-4.50345321311901	2.23807550616149

Radicaldeprotonated on indole

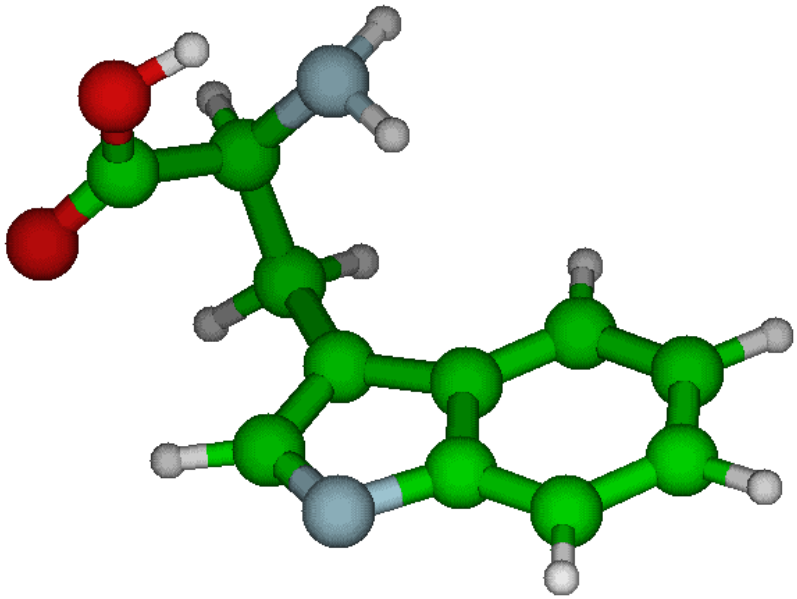

1 c	-0.14399216436251	0.50842154945102	-0.03919824937705
2 c	-0.03644979401436	0.40604404446206	2.61505809977940
3 c	2.28497868838626	0.06805471471604	3.73214240663618
4 c	4.51666560917663	-0.18716386060441	2.25443289327512
5 c	4.38599467816391	-0.06662086541039	-0.37714590284834
6 c	2.02628342959385	0.28287745588797	-1.50808380181139
7 n	2.84144790251473	-0.07284018741020	6.33392495058272
8 c	5.29055565996058	-0.40878203941865	6.47685147373494
9 c	6.51841579489535	-0.51241921855531	4.03989812913207
10 c	9.25177901517835	-0.93569607577472	3.53072872122946
11 c	10.04195752275183	-3.76000916688435	3.52470373134565
12 c	9.93776527435273	-4.88199655331522	6.21713853419435
13 o	10.56326474983761	-3.71719359897828	8.06481755622048
14 n	8.68923072831393	-5.40571571205835	1.75755347419808
15 o	9.17157770726546	-7.28713216542875	6.29958431545107
16 h	8.74364343778301	-7.73389736635430	4.55038909174738
17 h	12.04365864402009	-3.82416854960775	3.02288193166393
18 h	10.38747372436138	-0.00366180101754	4.97627856121609
19 h	9.76531771088272	-0.13175729078688	1.70183711788302
20 h	6.24451362584703	-0.58959235463069	8.27467902677772
21 h	6.06498663124129	-0.22068529535211	-1.53717552426497
22 h	-1.72495055581636	0.59112054525973	3.75101735954676
23 h	1.88341189006844	0.38616858980368	-3.54384736451026
24 h	-1.95122561908683	0.77597276491767	-0.95641006798322
25 h	9.51943405243206	-5.46530911272303	0.03954000996904
26 h	6.86882570047961	-4.86038892093263	1.52105854258898